

Article

Three-Dimensional Assessment of Upper Limb Proprioception via a Wearable Exoskeleton

Elisa Galofaro ^{1,2,*}, Erika D'Antonio ^{1,†}, Fabrizio Patané ³, Maura Casadio ² and Lorenzo Masia ^{1,4}

¹ Assistive Robotics and Interactive Exosuits (ARIES) Lab, Institute of Computer Engineering (ZITI), University of Heidelberg, 69120 Heidelberg, Germany; erika.dantonio@ziti.uni-heidelberg.de (E.D.); lorenzo.masia@ziti.uni-heidelberg.de (L.M.)

² Department of Informatics, Bioengineering, Robotics, and System Engineering (DIBRIS), University of Genoa, 16145 Genoa, Italy; maura.casadio@unige.it

³ Mechanical Measurements and Microelectronics (M3Lab) Lab, Engineering Department, University Niccolò Cusano, 00166 Rome, Italy; fabrizio.patane@unicusano.it

⁴ Maersk Mc-Kinney Moller Institute, Faculty of Engineering, University of Southern Denmark (SDU), 5230 Odense, Denmark

* Correspondence: elisa.galofaro@ziti.uni-heidelberg.de

† These authors have contributed equally to this work and share the first authorship.

Abstract: Proprioception—the sense of body segment’s position and movement—plays a crucial role in human motor control, integrating the sensory information necessary for the correct execution of daily life activities. Despite scientific evidence recognizes that several neurological diseases hamper proprioceptive encoding with consequent inability to correctly perform movements, proprioceptive assessment in clinical settings is still limited to standard scales. Literature on physiology of upper limb’s proprioception is mainly focused on experimental approaches involving planar setups, while the present work provides a novel paradigm for assessing proprioception during single—and multi-joint matching tasks in a three-dimensional workspace. To such extent, a six-degrees of freedom exoskeleton, ALEX-RS (Arm Light Exoskeleton Rehab Station), was used to evaluate 18 healthy subjects’ abilities in matching proprioceptive targets during combined single and multi-joint arm’s movements: shoulder abduction/adduction, shoulder flexion/extension, and elbow flexion/extension. Results provided evidence that proprioceptive abilities depend on the number of joints simultaneously involved in the task and on their anatomical location, since muscle spindles work along their preferred direction, modulating the streaming of sensory information accordingly. These findings suggest solutions for clinical sensorimotor evaluation after neurological disease, where assessing proprioceptive deficits can improve the recovery path and complement the rehabilitation outcomes.

Keywords: robot-aided assessment; wearable robotics; sensorimotor integration; kinaesthesia; proprioception; neurorehabilitation



Citation: Galofaro, E.; D’Antonio, E.; Patané, F.; Casadio, M.; Masia, L. Three-Dimensional Assessment of Upper Limb Proprioception via a Wearable Exoskeleton. *Appl. Sci.* **2021**, *11*, 2615. <https://doi.org/10.3390/app11062615>

Academic Editor: Matteo Laffranchi

Received: 25 February 2021

Accepted: 11 March 2021

Published: 15 March 2021

Publisher’s Note: MDPI stays neutral with regard to jurisdictional claims in published maps and institutional affiliations.



Copyright: © 2021 by the authors. Licensee MDPI, Basel, Switzerland. This article is an open access article distributed under the terms and conditions of the Creative Commons Attribution (CC BY) license (<https://creativecommons.org/licenses/by/4.0/>).

1. Introduction

Proprioception can be defined as the awareness of body segment positions and movements in the surrounding space [1]. Any change regarding a body district’s configuration activates mechanoreceptors located in joints, muscles, and tendons [2]. A key role in providing proprioceptive signals is played by the muscle spindles, the Golgi tendon organs, and the stretch receptors [3]. All the proprioceptive processes that promote awareness of body segment’s position are critical for the control of complex movement as well as posture [4].

Neurological injuries can significantly alter or deprive the central nervous system of peripheral sensory information [5], leading to a deterioration of the body awareness [6] and of the capacity to perform even a simple movement [7]. With neuropathies, despite gross motor functions are preserved [8], yet considerable sensorimotor deficits can persist [9].

In regular clinical practice, proprioceptive impairments receive less attention than motor deficits [10], and are usually quantified through clinical scales (Fugl–Meyer Assessment Scale [11] and Nottingham Sensory Assessment scale [12]), lacking in accuracy, precision, and reliability [13,14], and leading to incongruences and low agreement with clinical results obtained from imaging studies [10].

Scientific literature reports several attempts to provide quantitative measurements of proprioception [15–19]: Dukelow et al. adopted a planar robotic exoskeletal arm to quantify proprioception after stroke in a bidimensional workspace (2D) by means of a classic position matching task paradigm [20,21]. They passively moved the patients' impaired arm towards a target position, and successively asked them to mirror with the contralateral arm. Results provided evidence that proprioceptive sensitivity depends on both the arm's configuration and the movement direction. Other contributions [22–24] found that muscle spindles are sensitive to movements in different directions which are highly specific: each muscle shows a maximum sensitivity to a particular movement direction, i.e., the preferred sensory direction.

Further studies have shown that the central nervous system programs movements considering the gravity acting on the limb: arm kinematics changes for movements performed across different directions along the "vertical axis" (i.e., going upward or downward), coherently with the optimization of both inertial and gravitational forces [25–27]. Hence, in a three-dimensional workspace, proprioceptive sensitivity could be modulated by gravity's effects on the arm configuration.

Sketch et al. [28] used a planar robotic arm to analyse proprioceptive acuity in single-joint and multi-joint tasks, focusing on the elbow, shoulder, and hand, still limited to a 2D planar workspace.

Only recently, authors started to treat the evaluation of proprioception across a three-dimensional (3D) space: Marini et al. [29] characterized the wrist proprioception by considering each of the three degrees of freedom (DoFs), showing changes in proprioceptive acuity across different directions. Similarly, other researchers [30–33] started investigating how proprioception varies when single or multiple joints are involved in a motion task. However, in the latter cases, their evaluation was only conducted by analyzing the final arm position, by means of end-effector devices.

Recent advancements in exoskeleton's design provide the possibility of implementing proprioceptive paradigms involving a full-human range of motion, complementing with many DoFs to precisely determine the joint position [34–37]. Exoskeletons exhibit numerous advantages compared to the end-effector robots, in particular for upper limb proprioceptive assessment: they offer the possibility of implementing three-dimensional tasks, following the arm's natural workspace, and enabling for independent or simultaneous movement of the shoulder, elbow, and wrist joints.

Based on the references above, it is a consolidated opinion that proprioception is fed back considering both direction of motion and final arm configuration, and given the lack of studies that evaluate proprioceptive acuity along every single arm joint in a 3D-workspace, we decided to develop a spatial task for the assessment of proprioception, using a six DoFs bimanual exoskeleton, ALEx-RS [38,39]. Our protocol enables quantifying single and multi-joint position sense, involving an active matching movement of each upper limb.

The purpose of this study was to evaluate the "sensorimotor" contribution in single- or multi-joint arm movements (shoulder abduction/adduction, shoulder flexion/extension, and elbow flexion/extension) in healthy subjects, using an ipsilateral joint position matching (JPM) test. We aim at understanding (i) how proprioceptive acuity changes along the arm moving from proximal body joints to the distal ones; (ii) how the human nervous system decodes the simultaneous activation of more than one body joint (multi-joint).

2. Materials and Methods

2.1. Subjects and Experimental Setup

A group of eighteen healthy and right-handed subjects (8 females and 10 males, 27.94 ± 3.83 (mean \pm std) years old, range: 22–33 years) took part in this study. In the group, there was no significant difference in the age distribution between males and females. For all the subjects, we evaluated the handedness through the Edinburgh Handedness Questionnaire [40] (Laterality score (LS) = 81.89 ± 13.07 (mean \pm std), right-handed if $LS > 60$). All participants provided their informed consent. The experimental protocol was approved by the Heidelberg University Institutional Review Board (S-287/2020), and the study was conducted in accordance with the ethical standards of the Declaration of Helsinki. Experiments were carried out at the Aries Lab (Assistive Robotics and Interactive Exosuits) of the University of Heidelberg, Germany. Subjects self-reported no evidence or known history of neurological diseases and exhibited a normal joint range of motion and muscle strength.

The experimental design involved a task where subjects worn the bimanual Arm Light Exoskeleton Rehab Station ALEx-RS [38,39], shown in Figure 1A. An initial phase was run before starting the experiment to allow participants to familiarize with the device and its dynamics. Subjects wore a mask over their eyes to occlude vision during the whole experiment.

The device consists of two identical robotic exoskeletons with 6-DoFs for each side. Four DoFs are sensorized and actuated: shoulder abduction/adduction (AA_{Shoulder}), shoulder pronation/supination (PS_{Shoulder}), shoulder flexion/extension (FE_{Shoulder}) and elbow flexion/extension (FE_{Elbow}); the other two DoFs are only sensorized: wrist pronation/supination (PS_{Wrist}) and wrist flexion/extension (FE_{Wrist}). The latter was blocked during the experiment to avoid uncontrolled movements.

The range of motion (ROM) of each exoskeleton can approximately cover 92% of the upper limb workspace: the system is powered by a tendon-driven transmission system with low inertia and makes the overall structure highly transparent. Four brushless motors provided maximum torque values of 35 Nm for both AA_{Shoulder} and PS_{Shoulder} , 25 Nm for FE_{Shoulder} , and 20 Nm for FE_{Elbow} .

The controller of the device includes the possibility to use the workstation in 3 modalities: (i) “passive”, in which the subject individually moves her/his arms in a back driveable dynamic mode; (ii) “assistive”, in which the robot drives the upper limbs during the task execution; and (iii) “assisted-when-needed”, in which the robot guides the user’s arm when she/he is not able to initiate movements exceeding a time threshold. In all of the three modalities, the exoskeletons provide gravity and friction compensation, and the inertia is mostly cancelled by an inverse dynamic model running during operation and perceiving the user’s motion by the absorbed currents from the motors. In the framework of the current contribution, an impedance control has been adopted to allow the user to actively match the imposed target and being passively guided by the robot during the target presentation as described in the following section.

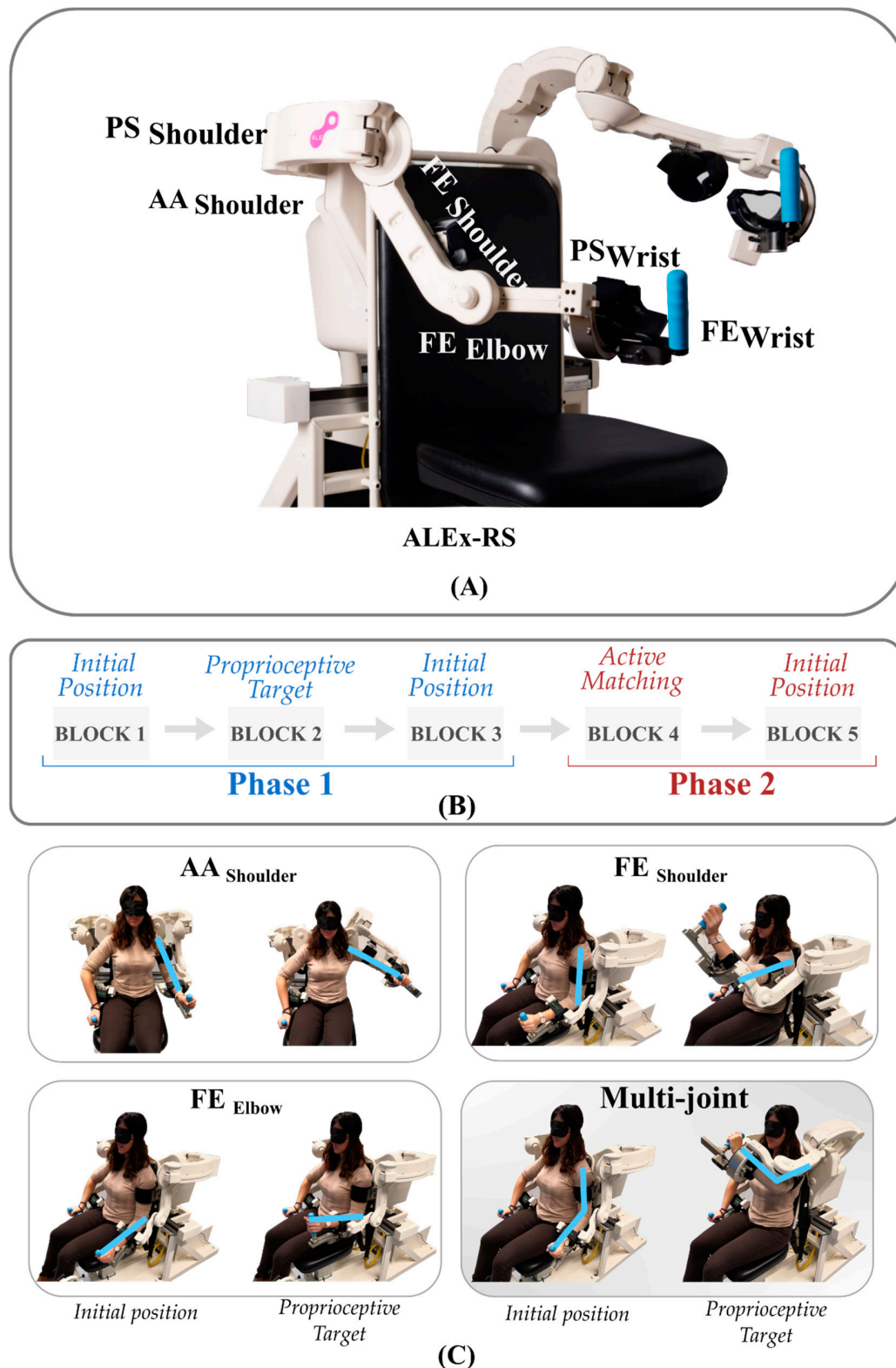


Figure 1. (A) Bimanual ALEx-RS device. (B) Block sequence presented to the participants during the ipsilateral joint position matching (JPM) task. (C) Task representation: participants sat on the workstation chair wearing one of the robotic exoskeletons, according to the tested body side. They were requested to grasp a pressure-sensitive handle of the contralateral exoskeleton (non-tested side). On the top left is illustrated the single joint (SJ) condition for the AA_{Shoulder}, on the top right for the FE_{Shoulder}, on the bottom left for the FE_{Elbow}. On the bottom right is illustrated the multi-joint (MJ) condition. For all conditions is shown the Initial Position on the left and the Proprioceptive Target position on the right.

2.2. Task and Procedure

During the experiment, participants sat on the workstation chair wearing one of the robotic exoskeletons, according to the tested body side. They were requested to grasp a pressure-sensitive handle of the contralateral exoskeleton (non-tested side). Arms and forearms were firmly strapped to ensure arm positioning's repeatability and limit inter-trial variability and undesired relative movements during the experiment.

The proprioceptive test consisted of an ipsilateral JPM task [9], involving a single trial with two main phases (Figure 1B):

1. Phase 1 or "Stimuli Presentation" in which the blindfolded user's arm was passively moved by the exoskeleton from an "Initial Position" ($AA_{Shoulder}: 10^\circ$, $FE_{Shoulder}: 5^\circ$ and $FE_{Elbow}: -40^\circ$) to a "Proprioceptive Target" ($AA_{Shoulder}: 60^\circ$, $FE_{Shoulder}: 80^\circ$ and $FE_{Elbow}: -10^\circ$). An auditory cue (high-frequency beep) was provided when the robot reached the Proprioceptive Target. Successively, after the target presentation, the robot moves back the users' arm to the initial posture (Block 3).
2. Phase 2 or "Active Matching" started with a sound and required the subjects to match, as accurately as possible, the previously experienced stimuli by actively moving her/his arm: this was possible because the exoskeleton was set in a transparent modality, i.e., without applying any force. Participants could stop the trial when matched position by squeezing the handle held in the contralateral hand (Block 4). After each trial's completion, the robot drove back the subject's arm to the initial position before initiating the next trial (Block 5), Figure 1B.

We tested the proprioceptive acuity in two different modalities:

- "Single Joint" (SJ): only one of the three examined degrees of freedom was independently tested for JPM task ($AA_{Shoulder}$ or $FE_{Shoulder}$ or FE_{Elbow}) (Figure 1C top).
- "Multiple Joints" (MJ): proprioceptive targets were presented by moving all the three degrees of freedom in a multi-joint fashion ($AA_{Shoulder} + FE_{Shoulder} + FE_{Elbow}$) (Figure 1C bottom).

The whole experimental session included four target sets (3 SJ and 1 MJ) for both left and right arms, which were pseudo-randomly distributed across participants in order to avoid possible target sequence effects. Each target sets counted 10 proprioceptive target presentations and the relative matching tasks. A total of 80 trials (30 SJ +10 MJ distributed on the two arms) were administered to each subject, with a 5-min break between each target set, for a total duration of about 1 h for the whole experiment.

2.3. Data Analysis

Trajectories were saved at 100 Hz frequency. Recorded joints' positions were filtered offline using a third order Savitzky–Golay low-pass filter (cut-off frequency of 10 Hz).

Proprioceptive performance was computed by using three kinematic indicators evaluated on the N repetition across each experimental condition (SJ and MJ):

1. The "Matching Error", which analyses performance accuracy, by computing the average of the absolute error between the proprioceptive target position ϑ_{target} and the arm configuration ϑ_i :

$$\text{Matching Error} = \frac{1}{N} \times \sum_{i=1}^N |\vartheta_i - \vartheta_{target}| \quad (1)$$

2. The "Error Bias" [4] evaluates the overshoot and undershoot during the matching task by considering the signed error between the presented proprioceptive target location (ϑ_{target}) and the final position (ϑ_i) at the end of each trial [41]. For consistent interpretation, we transformed the signed Error Bias to a measure of a signed overshoot:

$$\text{Error Bias}_{OS} = \frac{1}{N} \times \text{sign}(\vartheta_{target}) \times \sum_{i=1}^N (\vartheta_i - \vartheta_{target}). \quad (2)$$

In this outcome, negative values represent an undershoot, and positive values represent an overshoot independently of the sign of the presented proprioceptive target.

Both metrics have been expressed as percentage (%) of the distance between the Initial Position and the Proprioceptive Target which varied for each DoF considered ($\Delta\theta = 50^\circ$ for AA_{Shoulder}, $\Delta\theta = 75^\circ$ for FE_{Shoulder} and $\Delta\theta = 30^\circ$ for FE_{Elbow}). The target amplitudes were selected to reproduce in the MJ condition a typical functional gesture of daily activities, maintaining a percentage of about 30% of the total functional ROM for each DoF.

2.4. Statistical Analysis

Data normality was evaluated using the Shapiro–Wilk test, and sphericity condition for repeated measures analyses of variance (rANOVA) was assessed using the Mauchly test. The rANOVA test was used to examine the effects of the upper limb condition, the DoF, and the body's side on the dependent variables (Error Bias, and Matching Error). We considered three within-subject factors: (i) “condition” (2 levels: SJ and MJ), (ii) “DoF” (4 levels: AA_{Shoulder}, FE_{Shoulder}, FE_{Elbow}, and MJ), (iii) “Side” (2 levels: left and right) and their interaction. A post-hoc analysis was performed using the paired *t*-tests to evaluate the significant pairwise differences between each perturbation, DoF, and condition. All the tests have a statistical significance level set at 0.05, except for post-hoc analysis, where the significance level was reduced to 0.004 for Bonferroni corrections. Statistical analysis was conducted by using IBM SPSS Statistics 23.

3. Results

3.1. Multi-Joint Condition Leads to a Decrease of Proprioceptive Acuity Resulting in an Underestimation of the Matching Target

All participants were able to perform the experiments involving the two conditions and the multiple target sets.

However, performance was significantly different when considering the DoFs and the testing modality. In detail, Figure 2 illustrates the comparison between the two conditions (SJ versus MJ) for both the Error Bias (A) and the Matching Error (B): two main different behaviours were found between the SJ and MJ tests.

All subjects showed a tendency to overshoot the Proprioceptive Target when requested to perform the matching task in SJ condition with the elbow FE_{Elbow}.

Contrarily, the same joint (FE_{Elbow}) undershot when the MJ condition was presented for both left and right arms.

Furthermore, a significant deterioration of proprioceptive acuity was also inferred in multiarticular complex movements (MJ) rather than in single joint (SJ): this was true only for the distal joint of the arm FE_{Elbow}, while the proximal anatomical district AA/FE shoulder, provided similar results independently on the testing modality (SJ vs. MJ).

The aforementioned differences were confirmed by rANOVA test, highlighting a significant condition (SJ vs. MJ) effect (“condition”: Error Bias: $F(1,18) = 33.5$, $p < 0.001$; Matching Error: $F(1,18) = 30.5$, $p < 0.001$).

Ultimately, we statistically inferred across the two conditions, by a paired *t*-test post-hoc analysis, different behaviour of each tested DoF, and it has been found that only FE_{Elbow} DoF presents statistically significant differences (see Tables 1 and 2). Contrarily the other tested limb's joint, the shoulder, maintains statistically similar performance independently on the condition.

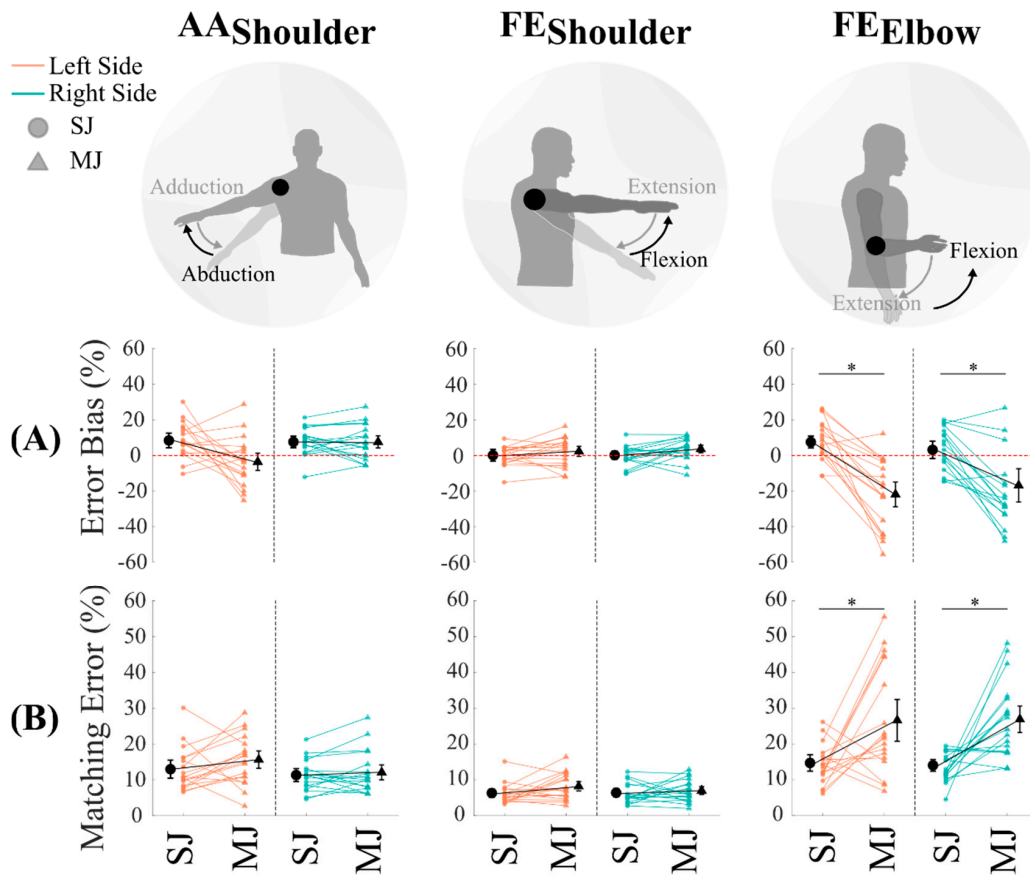


Figure 2. Outcome measures relative to the Error Bias and the Matching Error. In each graph, the orange color represents the left body side, while the green color represents the right one. The single-joint condition (SJ, which could be: AA_{Shoulder} or FE_{Shoulder} or FE_{Elbow}) is represented by a round marker, while a triangular marker represents the multi-joint condition (MJ). Black markers denote the averaged value between the subjects for each condition; the colored ones represent the mean value for each participant across the trials. Each column represents one DoF (AA_{Shoulder}, FE_{Shoulder}, and FE_{Elbow}). (A) Error bias. (B) Matching error. * represents the significant differences between the two conditions (SJ and MJ).

Table 1. Mean values and standard errors (%) for the Error Bias and Matching Error.

Body Side	DoF	Error Bias		Matching Error	
		SJ	MJ	SJ	MJ
Right	FE _{Elbow}	3.97 ± 2.75	-16.89 ± 6.26	13.24 ± 0.93	26.80 ± 2.49
	FE _{Shoulder}	0.37 ± 1.31	3.54 ± 1.42	6.12 ± 0.66	6.95 ± 3.12
	AA _{Shoulder}	7.53 ± 1.82	7.13 ± 2.28	11.21 ± 1.03	12.10 ± 1.40
Left	FE _{Elbow}	8.21 ± 2.67	-21.96 ± 4.67	14.01 ± 1.29	26.64 ± 3.59
	FE _{Shoulder}	-0.47 ± 1.29	2.31 ± 1.91	6.04 ± 0.66	8.08 ± 0.87
	AA _{Shoulder}	8.73 ± 2.32	-3.76 ± 3.26	12.94 ± 1.43	15.56 ± 1.63

Table 2. Statistical *p*-values for the Error Bias and Matching Error between conditions.

Body Side	Condition	Error Bias			Matching Error		
		FE _{Elbow}	FE _{Shoulder}	AA _{Shoulder}	FE _{Elbow}	FE _{Shoulder}	AA _{Shoulder}
Right	SJ						
	MJ	0.002 *	0.029	0.825	<0.001 *	0.379	0.335
Left	SJ						
	MJ	<0.001 *	0.112	0.012	0.002 *	0.051	0.172

* represents significant differences.

3.2. Proprioceptive Error Across Body Joints

We investigated another aspect of the proprioceptive performance across the different body segments and how their distal and proximal positions influence such performance in the body.

As depicted in Figure 2B, illustrating the Matching Error, for all conditions, it has been found a lower proprioceptive acuity for the distal body joint (elbow) than for the proximal one (shoulder).

The rANOVA test (Table 3), performed on the Error Bias and the Matching Error, highlighted a significant effect of the DoF (Error Bias: $F(2,18) = 8.6, p = 0.001$; Matching Error: $F(2,18) = 73.0, p < 0.001$) and an interaction effect between the conditions and the DoFs (Error Bias: $F(2,18) = 29.7, p < 0.001$; Matching Error: $F(2,18) = 17.2, p < 0.001$). No significant difference has been found between the body sides (Error Bias: $F(2,18) = 1.7, p = 0.213$; Matching Error: $F(2,18) = 1.5, p = 0.246$). The post-hoc analysis between the DoFs for the Error Bias and the Matching Error is reported in Table 3. The proprioceptive error resulted significantly larger for the distal joint than for the proximal one, considering the same DoF (FE).

Table 3. Statistical p -values for the Error Bias and Matching Error between the joints.

Body Side	DoF	Error Bias		Matching Error	
		SJ	MJ	SJ	MJ
Right	FE _{Elbow}				
	FE _{Shoulder}	0.173	0.014	<0.001 *	<0.001 *
	AA _{Shoulder}	0.289	0.006	0.197	0.002 *
	FE _{Shoulder}				
	AA _{Shoulder}	0.002 *	0.082	<0.001 *	<0.001 *
Left	FE _{Elbow}				
	FE _{Shoulder}	0.002 *	0.001 *	<0.001 *	<0.001 *
	AA _{Shoulder}	0.836	0.006	0.445	0.008
	FE _{Shoulder}				
	AA _{Shoulder}	0.001 *	0.127	0.001 *	<0.001 *

* represents significant differences.

4. Discussion

Despite the paramount importance of proprioception in sensorimotor control, studies investigating proprioceptive acuity in coordinated multi-joint setups are still limited to single-joint or confined in the execution of tests involving planar workspace. Furthermore, not much evidence can be found in the literature about experimentally assessed physiological aspects that rise from the interconnection between distal and proximal joints in the perception of proprioceptive targets. With this in mind, we aim at providing insights into how proprioceptive acuity is encoded at the multi-joint level by means of a novel experimental paradigm involving proprioceptive assessment via a robotic device.

We developed a protocol to compare “single”- versus “multi-joint” position matching in order to assess how perception of a proprioceptive target changes when multiple sensory information is encoded from the different sources or joints involved in the task.

We used a robotic setup to overcome previous limitations of planar setups and test subjects’ acuity of joints position across a 3D space.

The proposed paradigm aims not only at extending proprioceptive assessment to a multidimensional manifold, replicating complex arm configurations, but provided also the unprecedented possibility of studying in detail the interconnection between those anatomical joints responsible for covering the whole arm workspace. To the best of our knowledge,

there are no previous studies investigating such aspects involving robotic technology to increase measurement accuracy as well as contemplating a 3D testing paradigm.

It has been observed that proprioceptive performance is influenced by the number of joints involved in the task as well as by the anatomical configuration of the tested degrees of freedom [20,28,42].

4.1. Proprioceptive Acuity Differences between Single- and Multi-Joint Tasks

As evidenced by the performance indicators, the multi-joint condition leads to a decrease of proprioceptive acuity for the distal joint.

We want to support our results with the following considerations: (i) since MJ movements generally involve several processes required for stability, coordination, and neuromuscular control [43,44], their execution proves to be more complex than SJ ones; (ii) during the single-joint condition, the mechanoreceptors stimulation and the arising sensory information are better encoded by the central nervous system rather than when multiple information comes from different joints (MJ). In SJ condition, muscle spindles can work along their preferred direction by conveying their afferent information to the brain resulting in a population code representing the joint position [22–24]. Hence, in clinical settings, the sensory evaluation protocol should consider the number of joints simultaneously involved, modulating the obtained outcomes to the task complexity.

Moreover, our results have been extracted from an experimental setup involving a 3D-workspace and combining information arising from multiple peripersonal spatial components [45], and therefore introducing multiple factors: i.e., the gravity perception, which was involved in the dynamics of the task, and hence introducing extra-information in the sensory channel that complicates feedback integration when a MJ movement is required [25–27]. In contrast, Sketch et al. [28], who implemented a 2D-task, obtained a reverse result, evidencing that the MJ condition leads to lower matching errors than the SJ one. They justified their result, highlighting how MJ movements are more relevant from a “biological” point of view, i.e., they are closer to our routines compared to the SJ ones. However, the possibility to implement a 3D-scenario allowed us to cover the whole arm movement. In our study, subjects’ performance was compared across different workspaces, overcoming issues about how movements observed at the single-joint can be compared with their projection at the end-effector even though they have different metrics and dimensionality [46].

4.2. Proprioceptive Error across Upper Limb Joints

As previously discussed, our results highlighted a significant difference in proprioceptive acuity between the tested joints: in particular, regardless of experimental conditions (SJ or MJ), the largest matching error has been found in the distal district of the arm, the elbow. Our outcomes are consistent with the hypothesis that proprioceptive signals are differently encoded if they originate from proximal or distal segments. Brinkman and Kuypers [47] in a study on primates, highlighted the aspect mentioned above by experimentally demonstrating that the contralateral motor cortex is responsible for mediating distal movements, while motor commands related to proximal districts involve a neural activity from both the ipsilateral and contralateral motor cortex. Different neural pathways generate diverse motor behaviours as well as sensory processing between distal and proximal limbs, resulting in a significantly different performance between joints of the same limb. There is further evidence [42] demonstrating that in a 2D proprioceptive assessment, subjects’ performance was not isotropically distributed over the task workspace, but the largest errors have been found for more distal configurations of the limb.

Other studies confirmed that proprioceptive acuity is highly influenced by the configuration of the tested limb: performance in joint position matching tasks is worse for targets located in a distal portion of the arm workspace [16,41,48,49] rather than for those tested in proximal configurations [15,50,51].

The current work explores a unique multi-joint (MJ) configuration. The implementation of further MJ movements would help understand the proprioceptive mechanisms involved in a 3D-workspace to be included in a proprioceptive assessment protocol. Our findings provide the first proof of concept that can be considered to develop “evaluation protocols” and “ad-hoc rehabilitative interventions” for somatosensory retraining as published in recent works [52,53], also providing real-time feedback of the proprioceptive errors.

5. Conclusions

This study proposes a new paradigm using a robotic device for quantitatively assessing upper limb proprioception during a three-dimensional Joint Position Matching task.

The main finding can be summarized as the presence of a dissimilar proprioceptive acuity between joints of the same upper limb. In particular, the elbow and shoulder behave differently depending on the experimental condition and the arm configuration over the workspace.

The same robot-aided paradigm might be used in clinical settings. In fact, standard proprioceptive tests in medical practice provide assessments that are manually dispensed by the therapists, resulting in a qualitative low-resolution observation. Our findings may suggest that the use of robotic technology, which is rapidly and progressively spreading in hospitals and rehabilitation structures, might help clinicians in effectively evaluating proprioceptive deficits in a multi-joint fashion, thus drastically improving measurement accuracy and reliability. We hope that despite our investigation involves only an unimpaired sample population, it may arouse clinicians’ interest in the proposed paradigm in conjunction with the recent advancement in wearable technology, and invite the medical community to further pursue the use of robotics for clinical assessment.

Author Contributions: E.G. and E.D. conceived the idea and concept; they designed and implemented the experiment, acquired the data, analyzed and interpreted the data, and drafted the manuscript. F.P. and M.C. critically revised the manuscript content. L.M. critically revised the manuscript content, and supervised the study. All authors have read and agreed to the published version of the manuscript.

Funding: This research received no external funding.

Institutional Review Board Statement: The study was conducted according to the guidelines of the Declaration of Helsinki, and approved by the Institutional Review Board of Heidelberg University (S-287/2020).

Informed Consent Statement: The participants provided their written informed consent to participate in this study.

Data Availability Statement: The datasets generated and/or analyzed for this study are available from the corresponding author on reasonable request.

Acknowledgments: We acknowledge financial support by Deutsche Forschungsgemeinschaft within the funding programme Open Access Publishing, by the Baden-Württemberg Ministry of Science, Research and the Arts and by Ruprecht-Karls-Universität Heidelberg.

Conflicts of Interest: The authors declare that the research was conducted in the absence of any commercial or financial relationships that could be construed as a potential conflict of interest.

References

1. McCloskey, D.I. Kinesthetic sensibility. *Physiol. Rev.* **1978**, *58*, 763–820. [[CrossRef](#)] [[PubMed](#)]
2. Riemann, B.L.; Lephart, S.M. The sensorimotor system, part II: The role of proprioception in motor control and functional joint stability. *J. Athl. Train.* **2002**, *37*, 80.
3. Proske, U.; Gandevia, S.C. The proprioceptive senses: Their roles in signaling body shape, body position and movement, and muscle force. *Physiol. Rev.* **2012**, *92*, 1651–1697. [[CrossRef](#)] [[PubMed](#)]
4. Schmidt, R.A. *Motor Control and Learning: A Behavioral Emphasis*, 2nd ed.; Human Kinetics Publishers: Champaign, IL, USA, 1988; ISBN 1450412297.

5. Langhorne, P.; Coupar, F.; Pollock, A. Motor recovery after stroke: A systematic review. *Lancet Neurol.* **2009**, *8*, 741–754. [[CrossRef](#)]
6. Debert, C.T.; Herter, T.M.; Scott, S.H.; Dukelow, S. Robotic assessment of sensorimotor deficits after traumatic brain injury. *J. Neurol. Phys. Ther.* **2012**, *36*, 58–67. [[CrossRef](#)] [[PubMed](#)]
7. Mochizuki, G.; Centen, A.; Resnick, M.; Lowrey, C.; Dukelow, S.P.; Scott, S.H. Movement kinematics and proprioception in post-stroke spasticity: Assessment using the Kinarm robotic exoskeleton. *J. Neuroeng. Rehabil.* **2019**, *16*, 146. [[CrossRef](#)] [[PubMed](#)]
8. Schabrun, S.M.; Hillier, S. Evidence for the retraining of sensation after stroke: A systematic review. *Clin. Rehabil.* **2009**, *23*, 27–39. [[CrossRef](#)]
9. Goble, D.J. Proprioceptive acuity assessment via joint position matching: From basic science to general practice. *Phys. Ther.* **2010**, *90*, 1176–1184. [[CrossRef](#)] [[PubMed](#)]
10. Findlater, S.E.; Mazerolle, E.L.; Pike, G.B.; Dukelow, S.P. Proprioception and motor performance after stroke: An examination of diffusion properties in sensory and motor pathways. *Hum. Brain Mapp.* **2019**, *40*, 2995–3009. [[CrossRef](#)]
11. Gladstone, D.J.; Danells, C.J.; Black, S.E. The Fugl-Meyer assessment of motor recovery after stroke: A critical review of its measurement properties. *Neurorehabil. Neural Repair* **2002**, *16*, 232–240. [[CrossRef](#)]
12. Lincoln, N.B.; Jackson, J.M.; Adams, S.A. Reliability and revision of the Nottingham Sensory Assessment for stroke patients. *Physiotherapy* **1998**, *84*, 358–365. [[CrossRef](#)]
13. Lincoln, N.B.; Crow, J.L.; Jackson, J.M.; Waters, G.R.; Adams, S.A.; Hodgson, P. The unreliability of sensory assessments. *Clin. Rehabil.* **1991**, *5*, 273–282. [[CrossRef](#)]
14. Connell, L.A.; Tyson, S.F. Measures of sensation in neurological conditions: A systematic review. *Clin. Rehabil.* **2012**, *26*, 68–80. [[CrossRef](#)]
15. Fuentes, C.T.; Bastian, A.J. Where is your arm? Variations in proprioception across space and tasks. *J. Neurophysiol.* **2010**, *103*, 164–171. [[CrossRef](#)] [[PubMed](#)]
16. Wilson, E.T.; Wong, J.; Gribble, P.L. Mapping proprioception across a 2D horizontal workspace. *PLoS ONE* **2010**, *5*, e11851. [[CrossRef](#)]
17. Cressman, E.K.; Henriques, D.Y.P. Motor adaptation and proprioceptive recalibration. In *Progress in Brain Research*; Elsevier: Amsterdam, The Netherlands, 2011; Volume 191, pp. 91–99. ISBN 0079-6123.
18. Kenzie, J.M.; Semrau, J.A.; Hill, M.D.; Scott, S.H.; Dukelow, S.P. A composite robotic-based measure of upper limb proprioception. *J. Neuroeng. Rehabil.* **2017**, *14*, 114. [[CrossRef](#)] [[PubMed](#)]
19. Mrotek, L.A.; Bengtson, M.; Stoeckmann, T.; Botzer, L.; Ghez, C.P.; McGuire, J.; Scheidt, R.A. The Arm Movement Detection (AMD) test: A fast robotic test of proprioceptive acuity in the arm. *J. Neuroeng. Rehabil.* **2017**, *14*, 64. [[CrossRef](#)]
20. Dukelow, S.P.; Herter, T.M.; Moore, K.D.; Demers, M.J.; Glasgow, J.L.; Bagg, S.D.; Norman, K.E.; Scott, S.H. Quantitative assessment of limb position sense following stroke. *Neurorehabil. Neural Repair* **2010**, *24*, 178–187. [[CrossRef](#)]
21. Dukelow, S.P.; Herter, T.M.; Bagg, S.D.; Scott, S.H. The independence of deficits in position sense and visually guided reaching following stroke. *J. Neuroeng. Rehabil.* **2012**, *9*, 72. [[CrossRef](#)]
22. Bergenheim, M.; Ribot-Ciscar, E.; Roll, J.-P. Proprioceptive population coding of two-dimensional limb movements in humans: I. Muscle spindle feedback during spatially oriented movements. *Exp. Brain Res.* **2000**, *134*, 301–310. [[CrossRef](#)]
23. Jones, K.E.; Wessberg, J.; Vallbo, Å.B. Directional tuning of human forearm muscle afferents during voluntary wrist movements. *J. Physiol.* **2001**, *536*, 635–647. [[CrossRef](#)] [[PubMed](#)]
24. Roll, J.-P.; Bergenheim, M.; Ribot-Ciscar, E. Proprioceptive population coding of two-dimensional limb movements in humans: II. Muscle-spindle feedback during “drawing-like” movements. *Exp. Brain Res.* **2000**, *134*, 311–321. [[CrossRef](#)] [[PubMed](#)]
25. Le Seac'h, A.B.; McIntyre, J. Multimodal reference frame for the planning of vertical arms movements. *Neurosci. Lett.* **2007**, *423*, 211–215. [[CrossRef](#)]
26. Berret, B.; Darlot, C.; Jean, F.; Pozzo, T.; Papaxanthis, C.; Gauthier, J.P. The inactivation principle: Mathematical solutions minimizing the absolute work and biological implications for the planning of arm movements. *PLoS Comput. Biol.* **2008**, *4*, e1000194. [[CrossRef](#)]
27. Papaxanthis, C.; Pozzo, T.; Schieppati, M. Trajectories of arm pointing movements on the sagittal plane vary with both direction and speed. *Exp. Brain Res.* **2003**, *148*, 498–503. [[CrossRef](#)] [[PubMed](#)]
28. Sketch, S.M.; Bastian, A.J.; Okamura, A.M. Comparing proprioceptive acuity in the arm between joint space and task space. In Proceedings of the 2018 IEEE Haptics Symposium (HAPTICS), Francis, CA, USA, 25–28 March 2018; pp. 125–132.
29. Marini, F.; Squeri, V.; Morasso, P.; Konczak, J.; Masia, L. Robot-aided mapping of wrist proprioceptive acuity across a 3D workspace. *PLoS ONE* **2016**, *11*, e0161155. [[CrossRef](#)]
30. Klein, J.; Whitsell, B.; Artemiadis, P.K.; Buneo, C.A. Perception of arm position in three-dimensional space. *Front. Hum. Neurosci.* **2018**, *12*, 331. [[CrossRef](#)]
31. Valdés, B.A.; Khoshnam, M.; Neva, J.L.; Menon, C. Robot-Aided Upper-limb Proprioceptive Training in Three-Dimensional Space. In Proceedings of the 2019 IEEE 16th International Conference on Rehabilitation Robotics (ICORR), Toronto, ON, Canada, 24–28 June 2019; pp. 121–126.
32. Valdés, B.A.; Khoshnam, M.; Neva, J.L.; Menon, C. Robotics-assisted visual-motor training influences arm position sense in three-dimensional space. *J. Neuroeng. Rehabil.* **2020**, *17*, 1–11. [[CrossRef](#)]
33. D’Antonio, E.; Galofaro, E.; Zenzeri, J.; Patané, F.; Konczak, J.; Casadio, M.; Masia, L. Robotic Assessment of Wrist Proprioception During Kinaesthetic Perturbations: A Neuroergonomic Approach. *Front. Neurobot.* **2021**, *15*, 19.

34. Blumenschein, L.H.; McDonald, C.G.; O'Malley, M.K. A cable-based series elastic actuator with conduit sensor for wearable exoskeletons. In Proceedings of the 2017 IEEE International Conference on Robotics and Automation (ICRA), Singapore, 29 May–3 June 2017; pp. 6687–6693.
35. Sui, D.; Fan, J.; Jin, H.; Cai, X.; Zhao, J.; Zhu, Y. Design of a wearable upper-limb exoskeleton for activities assistance of daily living. In Proceedings of the 2017 IEEE International Conference on Advanced Intelligent Mechatronics (AIM), Munich, Germany, 3–7 July 2017; pp. 845–850.
36. Fitle, K.D.; Pehlivan, A.U.; O'Malley, M.K. A robotic exoskeleton for rehabilitation and assessment of the upper limb following incomplete spinal cord injury. In Proceedings of the 2015 IEEE International Conference on Robotics and Automation (ICRA), Seattle, WA, USA, 26–30 May 2015; pp. 4960–4966.
37. Gupta, A.; Singh, A.; Verma, V.; Mondal, A.K.; Gupta, M.K. Developments and clinical evaluations of robotic exoskeleton technology for human upper-limb rehabilitation. *Adv. Robot.* **2020**, *34*, 1023–1040. [\[CrossRef\]](#)
38. Pirondini, E.; Coscia, M.; Marcheschi, S.; Roas, G.; Salsedo, F.; Frisoli, A.; Bergamasco, M.; Micera, S. Evaluation of the effects of the Arm Light Exoskeleton on movement execution and muscle activities: A pilot study on healthy subjects. *J. Neuroeng. Rehabil.* **2016**, *13*, 1–21. [\[CrossRef\]](#)
39. Frisoli, A. Exoskeletons for upper limb rehabilitation. In *Rehabilitation Robotics*; Elsevier: Amsterdam, The Netherlands, 2018; pp. 75–87.
40. Oldfield, R.C. The assessment and analysis of handedness: The Edinburgh inventory. *Neuropsychologia* **1971**, 97–113. [\[CrossRef\]](#)
41. Galofaro, E.; Ballardini, G.; Boggini, S.; Foti, F.; Nisky, I.; Casadio, M. Assessment of bimanual proprioception during an orientation matching task with a physically coupled object. In Proceedings of the 2019 IEEE 16th International Conference on Rehabilitation Robotics (ICORR), Toronto, ON, Canada, 24–28 June 2019; pp. 101–107.
42. Rincon-Gonzalez, L.; Buneo, C.A.; Tillery, S.I.H. The proprioceptive map of the arm is systematic and stable, but idiosyncratic. *PLoS ONE* **2011**, *6*, e25214. [\[CrossRef\]](#)
43. Kraemer, W.J.; Ratamess, N.A. Fundamentals of resistance training: Progression and exercise prescription. *Med. Sci. Sports Exerc.* **2004**, *36*, 674–688. [\[CrossRef\]](#)
44. Schwelanus, M.P. *The Olympic Textbook of Medicine in Sport*; John Wiley & Sons: Hoboken, NJ, USA, 2009; Volume 14, ISBN 1444300644.
45. Noel, J.-P.; Samad, M.; Doxon, A.; Clark, J.; Keller, S.; Di Luca, M. Peri-personal space as a prior in coupling visual and proprioceptive signals. *Sci. Rep.* **2018**, *8*, 1–15. [\[CrossRef\]](#)
46. Hansen, E.; Grimme, B.; Reimann, H.; Schöner, G. Carry-over coarticulation in joint angles. *Exp. Brain Res.* **2015**, *233*, 2555–2569. [\[CrossRef\]](#) [\[PubMed\]](#)
47. Brinkman, J.; Kuypers, H. Cerebral control of contralateral and ipsilateral arm, hand and finger movements in the split-brain rhesus monkey. *Brain* **1973**, *96*, 653–674. [\[CrossRef\]](#) [\[PubMed\]](#)
48. Iandolo, R.; Squeri, V.; De Santis, D.; Giannoni, P.; Morasso, P.; Casadio, M. Proprioceptive bimanual test in intrinsic and extrinsic coordinates. *Front. Hum. Neurosci.* **2015**, *9*, 1–11. [\[CrossRef\]](#)
49. Adamo, D.E.; Martin, B.J. Position sense asymmetry. *Exp. Brain Res.* **2009**, *192*, 87–95. [\[CrossRef\]](#) [\[PubMed\]](#)
50. Janwantanakul, P.; Magarey, M.E.; Jones, M.A.; Dansie, B.R. Variation in shoulder position sense at mid and extreme range of motion. *Arch. Phys. Med. Rehabil.* **2001**, *82*, 840–844. [\[CrossRef\]](#)
51. Tripp, B.L.; Uhl, T.L.; Mattacola, C.G.; Srinivasan, C.; Shapiro, R. A comparison of individual joint contributions to multijoint position reproduction acuity in overhead-throwing athletes. *Clin. Biomech.* **2006**, *21*, 466–473. [\[CrossRef\]](#) [\[PubMed\]](#)
52. Wang, Y.; Zhu, H.; Elangovan, N.; Cappello, L.; Sandini, G.; Masia, L.; Konczak, J. A robot-aided visuomotor wrist training induces gains in proprioceptive and movement accuracy in the contralateral wrist. *Sci. Rep.* **2021**, *11*, 5281. [\[CrossRef\]](#) [\[PubMed\]](#)
53. Elangovan, N.; Cappello, L.; Masia, L.; Aman, J.; Konczak, J. A robot-aided visuo-motor training that improves proprioception and spatial accuracy of untrained movement. *Sci. Rep.* **2017**, *7*, 1–10. [\[CrossRef\]](#) [\[PubMed\]](#)